REVIEW OF HIGH INTENSITY H⁻ SOURCES AND MATCHING TO HIGH – POWER RFQ´S

J. Peters, DESY, Hamburg, Germany

Abstract

Due to the development of reliable H⁻ ion sources, charge-exchange injection into circular accelerators has become routine. This paper reviews recent developments in negative hydrogen ion sources. The underlying physics, operating parameters and beam characteristics of selected sources will be described and compared. The matching to the RFQ is done with a low energy beam transport line (LEBT). Different kinds of transport lines with magnetic and electrical focussing are presented. and compared.

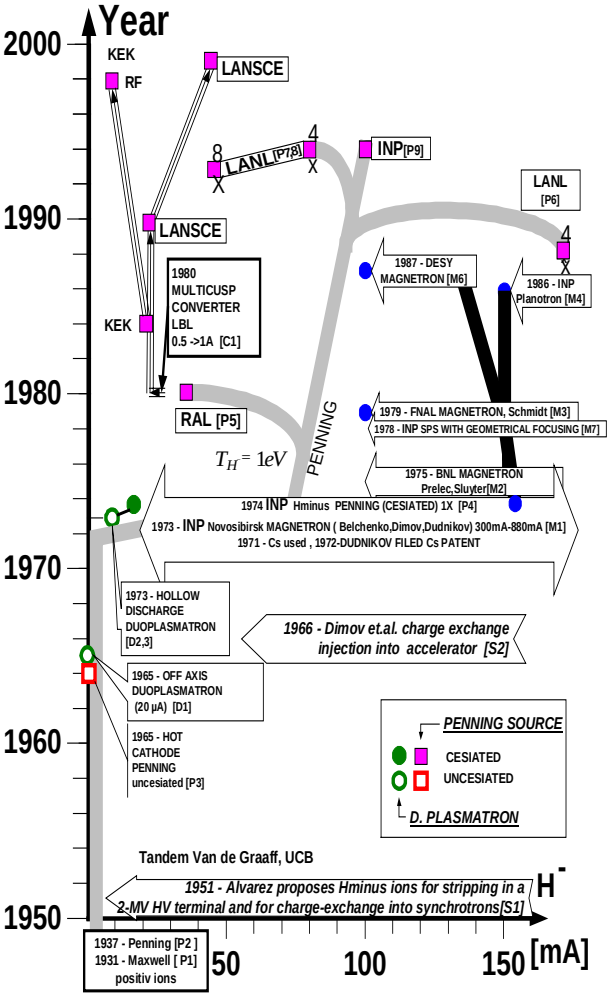

Figure 1: History of duoplasmatron and surface source development.

1 INTRODUCTION

This paper will deal primarily with H⁻ sources used as injectors for high energy accelerators. Usual (high) H⁻ currents are 10 to 120 mA dependent on the duty factor. It has taken two decades to reach these currents since Alvarez proposed H⁻ ions for stripping in a high voltage terminal and for charge-exchange injection into synchrotrons (Fig.1 S1) [1].
Duoplasmatrons (D1,2,3) with their low currents are excluded as well as multi aperture sources which have high currents but low brightness .

1.1 Definition of brightness and emittance

Several definitions of brightness are in use. The following relation is adopted here :

$$B = \frac{I}{\varepsilon^{N}_{x,90\%}\ \varepsilon^{N}_{y,90\%}} \quad ,$$

where $\varepsilon^{N}_{x,90\%}$ is the energy normalized emittance in the (x ,x') plane for the contour containing 90% of the brightest beam and

$$\varepsilon^{N} = \varepsilon\ \beta\ \gamma \quad ,$$

with : $\beta = v_{BEAM}/c$ and $\gamma = 1/(1-\beta^2)^{1/2}$.
In the ideal case the contour is an ellipse and ε is the product of the semimajor and semiminor axes times π. Emittances quoted in conventions other than 90% area values can be converted using the following equations :
$\varepsilon_{90\%} = 4.6\ \varepsilon_{rms}$ and $\varepsilon_{90\%} = 1.125\ \varepsilon_{4rms}$ assuming a Gaussian distribution.

1.2 Emittance scanners and emittance errors

Emittance values found in the literature may differ very much even for the same source type and current. For this paper the labs were asked for emittances and the related current, type of emittance scanner, distance from scanner to extractor and other relevant source data. Most labs now use slit-multiwire scanners [DESY, BNL, RAL] or electrostatic sweep scanners (Allison) [LANL, LBL]. These devices are able to measure rms and area emittances. The pepperpot is also still in use. It measures only area emittances. In recently published emittance collections [2] area definitions have been used.

2 SURFACE SOURCES (SPS)

After the discovery of cesiation of surfaces at INP in 1971, the attainable H^- currents increased dramatically. The magnetron was invented (see Fig.1 M1)[3] and the penning source developed to its present standard (P4) [4] in Novosibirsk at INP .

2.1 Magnetron

Magnetron technology was transferred from INP to BNL (M2) [5] and from there to FNAL (M3) [6]. There was a mutual exchange between these two labs. In 1987 magnetron plans were brought from FNAL to DESY.

Figure 2 shows the structure of a magnetron in front and side views. It consists of a central cylindrical cathode surrounded by an anode. The discharge voltage, U_D , is typically ≈ 150 V and the current 40 A. A magnetic field

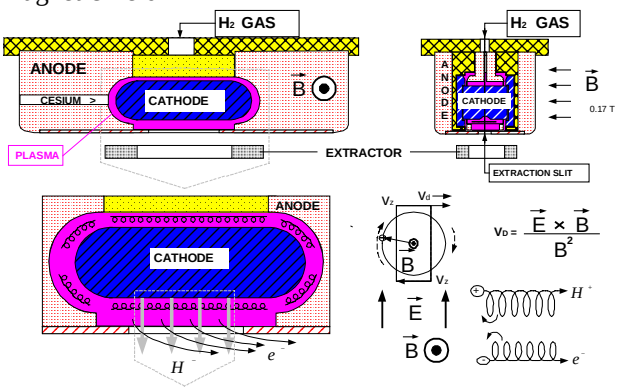

Figure 2: Magnetron source and E×B drift.

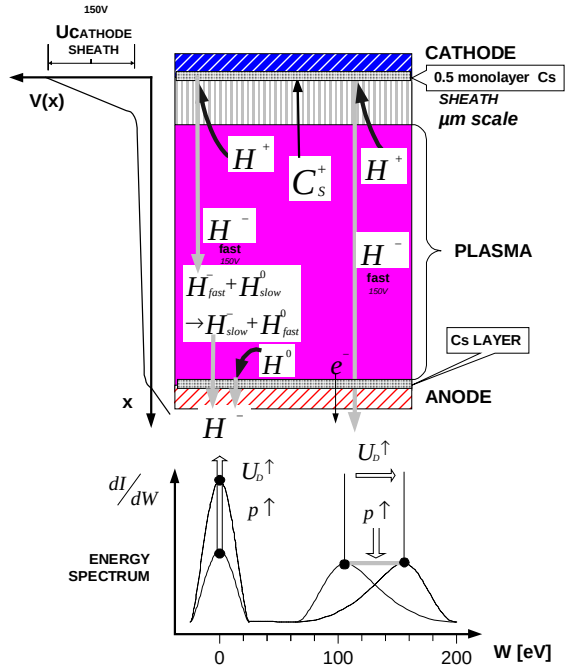

Figure 3: Production of H^- at cathode and anode of the source and their energy spectrum.

(≈ 0.17 T) is parallel to the cathode axis. Hydrogen gas is introduced from the top by a pulsed gas valve. Cesium is obtained by heating metallic cesium or a mixture of cesium chromate and titanium.The mixture is available as pellets or powder.

H^- ions are extracted at 18 kV (FNAL, DESY) or 35 kV (BNL) together with electrons. Modern magnetrons have geometric focussing, developed at INP in 1978, with a groove in the cathode and slit extraction followed by a bending magnet [7]. Another possibility is to dimple the cathode and to use a hole as aperture toward the extractor electrode [8].

The electric field between anode and cathode leads to an E×B drift around the cathode, which is shown on a magnified scale Fig.2 (lower part). Positive and negative ions move in the same direction. There is no movement parallel to E as particles gain as much energy as they lose. But parallel to E×B there is a resulting difference v_d (see Fig.2). Charges are not separated due to this effect. A dense plasma is produced.

If one looks with a bigger magnification at the space between anode and cathode (Fig. 3) one notices a transition zone, the so-called sheath, between the plasma and the cathode. Here the potential drops to cathode level. There is only a small potential difference across the plasma. H^+ ions generated in the plasma are accelerated through the sheath. They produce H^- ions at the cathode surface, which is covered in the ideal case with half a mono layer of Cs in order to minimize the surface work function. These H^- particles are then accelerated to U_D passing through the sheath. Some move through the plasma and are extracted. They form a maximum in the energy spectrum (Fig.3 lower part). Others hit slow H^0 particles and exchange speed and charge; this is resonant charge exchange. In this way slow H^- ions are produced. Slow H^- can also be produced by H^0 hitting the cesiated anode surface.

Due to these mechanisms a low and a high energy peak appear in the energy spectrum. To increase the fraction of low temperature ions one can increase the source pressure and discharge voltage U_D, as indicated in the plot. In addition, the position of the high energy peak can be changed by varying U_D and the amplitude lowered by increasing the pressure.

2.3 Penning

In order to avoid the high energy peak of the magnetron spectrum the cathode surface should not face the ion extraction aperture. This is how the penning source is constructed (see Fig. 4).

A strong magnetic field parallel to the electric field of the sheath guides electrons and ions on cyclotron spirals from cathode to cathode. Fast H^- ions are generated at the

cathodes as in the magnetron. They are slowed down

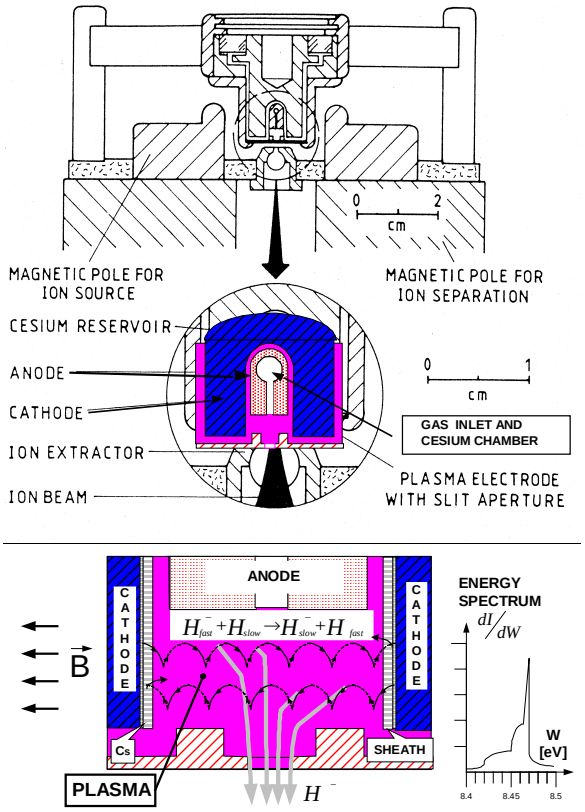

Figure 4: Penning source schematic and its energy spectrum

due to the charge exchange reaction as they migrate to the plasma aperture. There is only one low energy peak and the H^- temperature has been measured to be less than 1eV [9].

2.4 Multicusp Surface-plasma (converter) source

Fig. 5 shows a multicusp surface-plasma source. A discharge is produced with filaments. The plasma is confined by a multicusp field. A converter biased at ≈ -300 V is located in the middle of the source. Secondary emission of negative ions from a sputtered adsorbate film takes place. The H^- ions are produced by H^+, H_2^+ and H_3^+ bombarding the converter. Cesium is injected into the source to increase the H^- yield. Self extraction of H^- takes place with focussing provided by the curvature of the converter. A magnetic filter is used to repel electrons.

3 VOLUME SOURCES

In 1977 M. Bacal [10] discovered volume production for H^- generation. This started the development of a new type of sources (Fig. 6). The volume source consists of two chambers, which are connected by a magnetic filter (Fig. 7). In the high temperature chamber energetic electrons hit H_2, which become vibrationally excited.

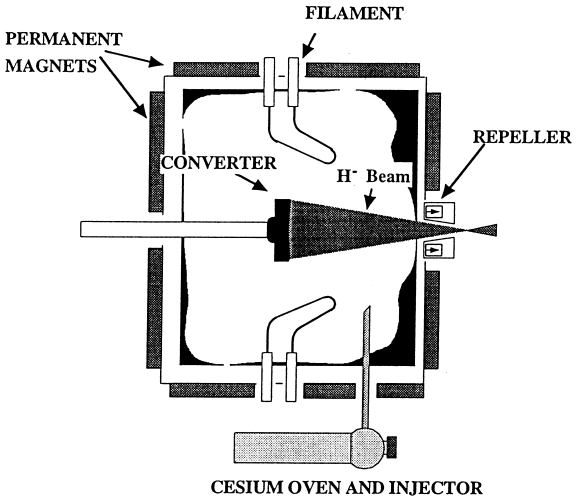

Figure 5: LANL surface production multicusp source

Excited molecule are also produced at the chamber walls out of H_2^+ and H^+. Electrons from the high temperature chamber move by diffusion through a perpendicular

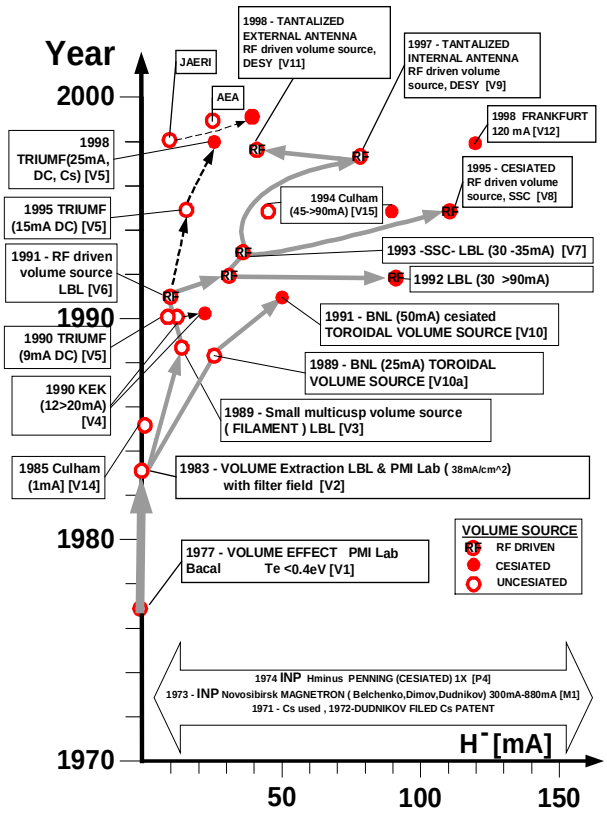

Figure 6 : History of volume source development

magnetic field into a second chamber. Whereas high energy electrons are effectively blocked, slow electrons collect in the second chamber. In this low energy chamber, low temperature 1eV electrons attach to the H_2^*

3.1 Filament Volume Source

The first volume sources were uncesiated and had filaments. Currents of up to 20mA DC [11] were reached

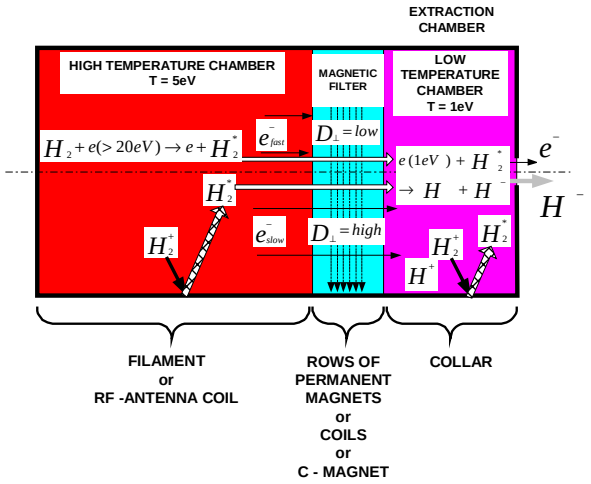

Figure 7 : Tandem source for volume production

with small sources and 45 mA [12] (Fig. 6 V15) with larger ones. Cesiated currents of 25 mA DC [13] and 90-120 mA at 6% duty factor [12,14] V12 have been achieved. The lifetime of these sources is limited by that of the filament.

3.2 RF Volume Source

The filament was first replaced by an rf antenna coil in 1991 [15]. The antenna heats the high temperature chamber and the filter is constructed with two rows of permanent magnets. The low temperature chamber is located inside a collar. The antennae are coated to reduce plasma modulation by the rf voltage and sputtering.

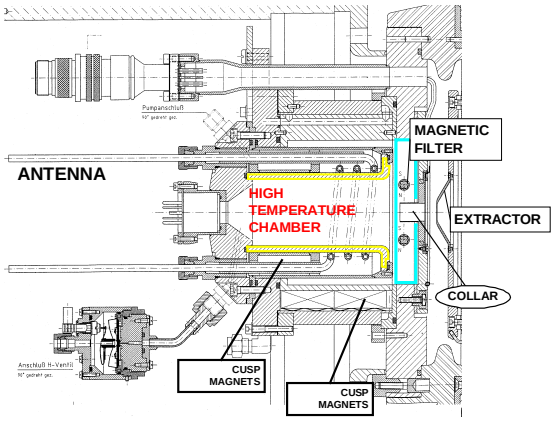

Figure 8. The DESY volume source with an rf coil shielded by $Al_2 O_3$ ceramic.

With uncesiated rf volume sources 35 mA has been reached.

At DESY with the collar biased and tantalum coated, currents of 80 mA were achieved uncesiated.

The antennae used by LBL, SSC and DESY were all coated by the same manufacturer. An analysis of the coating found a high percentage of K (15%) and Na (3%). Different contents of potassium might have contributed to reported differences in source performance.

The average lifetime of only 41 days is higher than that of a filament. However ≈ 50% of all antennae fail during the first 15 days. Even with their superior beam quality, this poor reliability would rule out the use of rf volume sources in injection systems for high energy accelerators.

A new rf coupling was then developed, which couples through a ceramic of $Al_2 O_3$. This type of ceramic has a sputter rate seven times lower than that of glass and three times lower than Ti (see Fig. 8).

4 MATCHING TO RFQ´S

H^- sources deliver a divergent beam of 100-140 mrad. A convergent round beam of 50 -100 mrad and an emittance $\varepsilon^N_{90\%}$ = 1 π mm mrad is necessary at the entrance of the RFQ. The matching is done by a low energy beam transport line (LEBT) which can have electric or magnetic focussing. The LEBT also provides space for pumping , diagnostics, chopper and an e^- dump. Usually the dumping is done in the source with a magnetic dipole. Magnetic LEBT systems have been often constructed out of two solenoids with two horizontal and

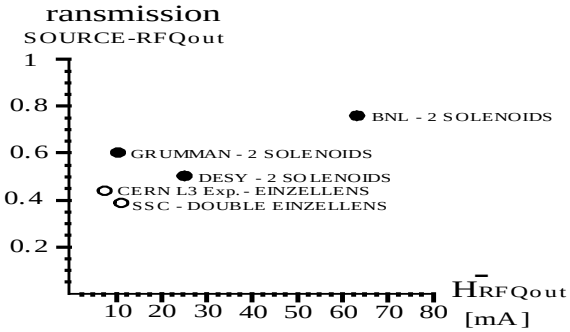

Figure 9. Transmission (source-RFQout)

vertical steerers. The tube diameter is about 0.1m and the length less than 1.4 m. The beam alignment tolerances are ±0.25 mm and ±10 mrad [16]. The rest gas in the transport line is ionised by the H^- beam and is pulled into the beam, reducing the space charge forces. The benefit comes only after a built up time of the plasma of some 10 μsec. A disadvantage is possible plasma oscillations if a source has more than 2% [16] noise. Magnetic systems (see Fig. 9) demonstrate the highest transmission (source-RFQout) [17] and the highest current. Electrical systems have been built with einzellenses [18], double einzellenses [19], [20], quadrupoles [21] and helical quadrupoles (HESQ) [22],[23]. They are short

Table 1: Collection of source data

tested uninter-rupted run[h]	**SOURCE TYPE**	**DUTY FACTOR** [%]	$\varepsilon^{N}_{90\%}$ [π mm mrad]	R E F.	**BRIGHT-NESS** [mA/mm^2 mrad^2]	C_s **CONS.** [mg/day]	**CURRENT** [I/mA]
7224 4320	MAGNETRON 17 yrs acc. exp.	0.05 0.48	0.98 1.2	[25a] [25b]	6.4 4.9	2.8	60 (->120) 75
960	PENNING. 16 yrs. acc. exp	2.5 2.5	0.3 0.1	[25c] [25d]	 670	 24	35(->170 [ref.25e]) 80
720	CONVERTER	12	0.53	[25e]	5.8	480	16-{45}
500	VOLUME Filament 10 yrs acc. exp.	100	0.75	[25f]	3.6	NO Cs	20
	Filament	100 6	0.52(0.6) ≈ 0.23	[25f] [25g]		5 29	20 (25) 120
72-984	RF Antenna in Plasma	0.1	0.5	[25h] [25i]	12	NO Cs but K	30 80
	RF Antenna inPlasma	0.1	0.5	[25j]	28	Cs	91 (->120)
2800	RF Antenna out of Plasma	0.05	0.75	[25i]	7.2	NO Cs	40

(l~0.2 m) and do not have time dependent focussing of space charge neutralisation as the positive ions are neutralised at the electrodes. In these systems chromatic aberrations can be a problem. There is no accelerator experience with quadrupole systems. So far current and transmission (source-RFQout) of electrical systems have been low (see Fig. 9). The new SNS system delivers a current of 46 mA at RFQ entrance [24]. Coupling to the RFQ will be the next step.

SUMMARY

A summary of sources is given in table 1, a summary of LEBT transmissions in Fig. 11 .

REFERENCES

[1] L.W.Alvarez,Rev.Sci.Instrum. 22,705(1951)
[2] J. R. Alonso, Rev. Sci. Instrum., Vol. 67, No.3, March 1996
[3] Yu.I.Belchenko, G.I.Dimov, V.G.Dudnikov, NUCLEAR FUSION 14 (1974)
[4] V.G.Dudnikov, Proc. IV All-Union Conf. On Charged Particle Accelerators, Moscow, 1974,Nauka 1975, Vol 1, p. 323
[5] K.A.Prelec,Th.Sluyters,M.Grossman,IEEE Trans.Nuc.Sci. NS-24(1977) 1521
[6] C.W.Schmidt, C.D.Curtis, IEEE Trans. Nuc. Sci. NS-26 (1979) 4120}
[7] C.W.Schmidt, Proceedings of LINAC90, Albuquerque, New Mexico, September 10-14, 1990, 259-263 (1990).
[8] J.G.Alessi et al., BNL – 42426, ICIS 1989, Lawrence Berkeley Lab, July 10-14, 1989
[9] J.D.Sherman et al., Rev. Sci. Instrum. 62 (10), October 1991
[10] M. Bacal et al., Phys. Rev. Lett. 42 1538, J.Phys. (Paris) 38, 1399 (1977)
[11] T. Kuo et al.,Rev. Sci. Instrum. 67 (3), March, 1996 and private communication
[12] A.J.T.Holmes et al, Rev. Sci. Instrum. 65 (4), April 1994
[13] private communication with T. Kuo , TRIUMF
[14] private communication with K. Volk and A. Maser, FRANKFURT UNIVERSITY
[15] K.N.Leung, G.J.DeVries, W.F.DiVergilio and R.W.Hamm, Rev.Sci.Instrum.62(1),100(1991)
[16] R.R.Stevens et al, Dallas workshop 1992 R.R.Stevens, AIP Conf. Proc. No.287, p. 646
[17] J.G. Alessi et al, Upgrade of the Brookhaven 200MeV Linac, page 773, LINAC 96
[18] private communication B.Ham, AccSys
[19] J.W.Lenz,J.Hebert,N.Okay, D.Raparia, K.Saadatmand, 1993 PAC Washington D.C
[20] ICFA newsletter 0004, April 2000
[21] S.K.Guharay et al, Rev.Sci.Instrument. 65 (5), May 1994
[22] Y.Mori et al, Dallas workshop 1992
[23] D.Raparia Proceedings 1990 LINAC Conf.
[24] private communication R. Thomae,LBL, 2000
[25] private communication with a) DESY, b) BNL, c) RAL, d) BINP, e) LANL, f) TRIUMF, g) FRANKFURT UNIVERSITY, h) LBL, i) DESY, j) SSC